Supplementary figure 1. 2D structure of the 150 known SARS-CoV-2 M-pro inhibitors extracted from the bibliography. Covalent warheads are highlighted in red. 2D structures were drawn from the SMILES using the RDKit library.

Supplementary figure 2. 2D structure of the 81 SARS-CoV-2 M-pro inhibitors from the COVID Moonshot project used for validation. Covalent warheads are highlighted in red. 2D structures were drawn from the SMILES using the RDKit library.

Supplementary figure 3. 2D structure of the 113 compounds from the COVID Moonshot project that are inactive against SARS-CoV-2 M-pro and which were used for validation. Covalent warheads are highlighted in red. 2D structures were drawn from the SMILES using the RDKit library.

Supplementary figure 4. Correlation between the highest docking scores from five different docking methods (FRED, Glide HTVS, Glide SP, Glide XP and AutoDock Vina) and the experimental inhibitory activity, measured as pIC_{50}, of a group of 150 M-pro inhibitors extracted from the literature (A-E) and 81 M-pro inhibitors from the COVID Moonshot project (F-J). The protein from the 6WQF PDB structure was used for docking. Data has been adjusted to a linear regression and the correlation coefficient is displayed in gray. Covalent and non-covalent inhibitors are also represented separately in orange and blue, respectively.

Supplementary figure 5. Correlation between the binding energy, calculated as the ΔG of the MM-GBSA method, and the experimental inhibitory activity, measured as pIC_{50}, of a group of 150 M-pro inhibitors extracted from the literature (A-E) and 81 M-pro inhibitors from the COVID Moonshot project (F-J). The protein from the 6WQF PDB structure was used for docking. The poses with the highest docking scores from each of the five different docking methods (FRED, Glide HTVS, Glide SP, Glide XP and AutoDock Vina) were used as the input to the MM-GBSA program to estimate the binding energy. Data has been adjusted to a linear regression and the correlation coefficient is displayed in gray. Covalent and non-covalent inhibitors are also represented separately in orange and blue, respectively.

Supplementary figure 6. ROC curves obtained from the docking scores of five different docking methods (FRED, Glide HTVS, Glide SP, Glide XP and AutoDock Vina) (A-E) and the ΔG calculated with the MM-GBSA program (F-J) of a group of known SARS-CoV-2 M-pro inhibitors and compounds with no activity against M-pro from the COVID Moonshot initiative. The protein from the 6WQF PDB structure was used for docking. Covalent, non-covalent and the whole set of inhibitors are represented separately. The area under the curve (AUC) values are displayed for each group.

Supplementary figure 7. Correlation between the pIC_{50} and the ΔG values estimated with the KDeep server from the best docking poses from five different docking methods (FRED, Glide HTVS, Glide SP, Glide XP and AutoDock Vina) (A-E) and the 6WQF M-pro structure of a group of 40 non-covalent SARS-CoV-2 M-pro inhibitors that were co-crystallized with the SARS-CoV-2 M-pro protein.

Figure S1

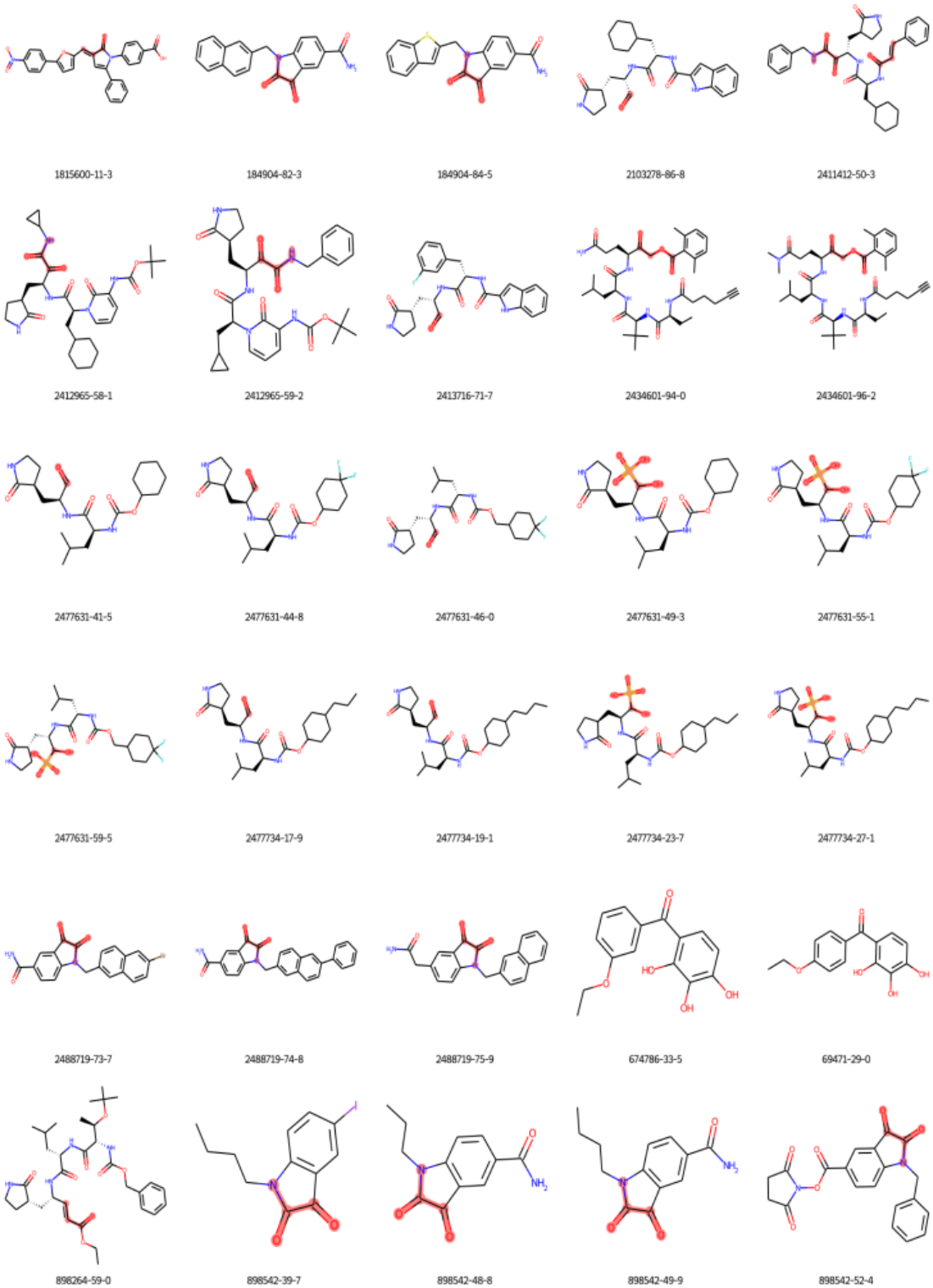
1815600-11-3
184904-82-3
184904-84-5
2103278-86-8
2411412-50-3
2412965-58-1
2412965-59-2
2413716-71-7
2434601-94-0
2434601-96-2
2477631-41-5
2477631-44-8
2477631-46-0
2477631-49-3
2477631-55-1
2477631-59-5
2477734-17-9
2477734-19-1
2477734-23-7
2477734-27-1
2488719-73-7
2488719-74-8
2488719-75-9
674786-33-5
69471-29-0
898264-59-0
898542-39-7
898542-48-8
898542-49-9
898542-52-4
Page 1 of 5

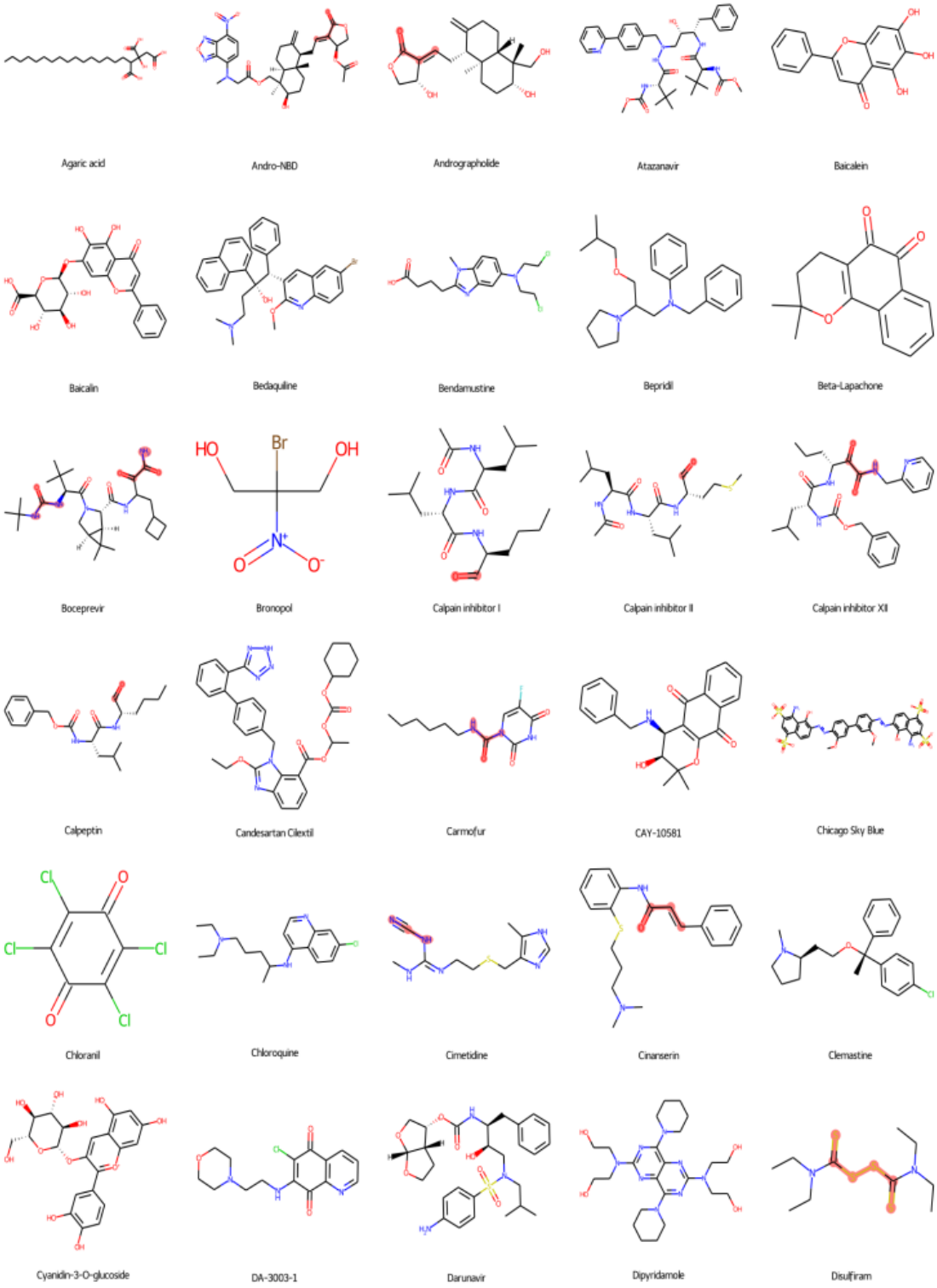
Agaric acid
Andro-NBD
Andrographolide
Atazanavir
Baicalein
Baicalin
Bedaquline
Bendamustine
Bepridil
Beta-Lapachone
Boceprevir
Bronopol
Calpain inhibitor I
Calpain inhibitor II
Calpain inhibitor XII
Calpeptin
Candesartan Cilextil
Carmofur
CAY-10581
Chicago Sky Blue
Chloranil
Chloroquine
Cimetidine
Cinanserin
Clemastine
Cyanidin-3-O-glucoside
DA-3003-1
Darunavir
Dipyridamole
Disulfiram

Page 2 of 5

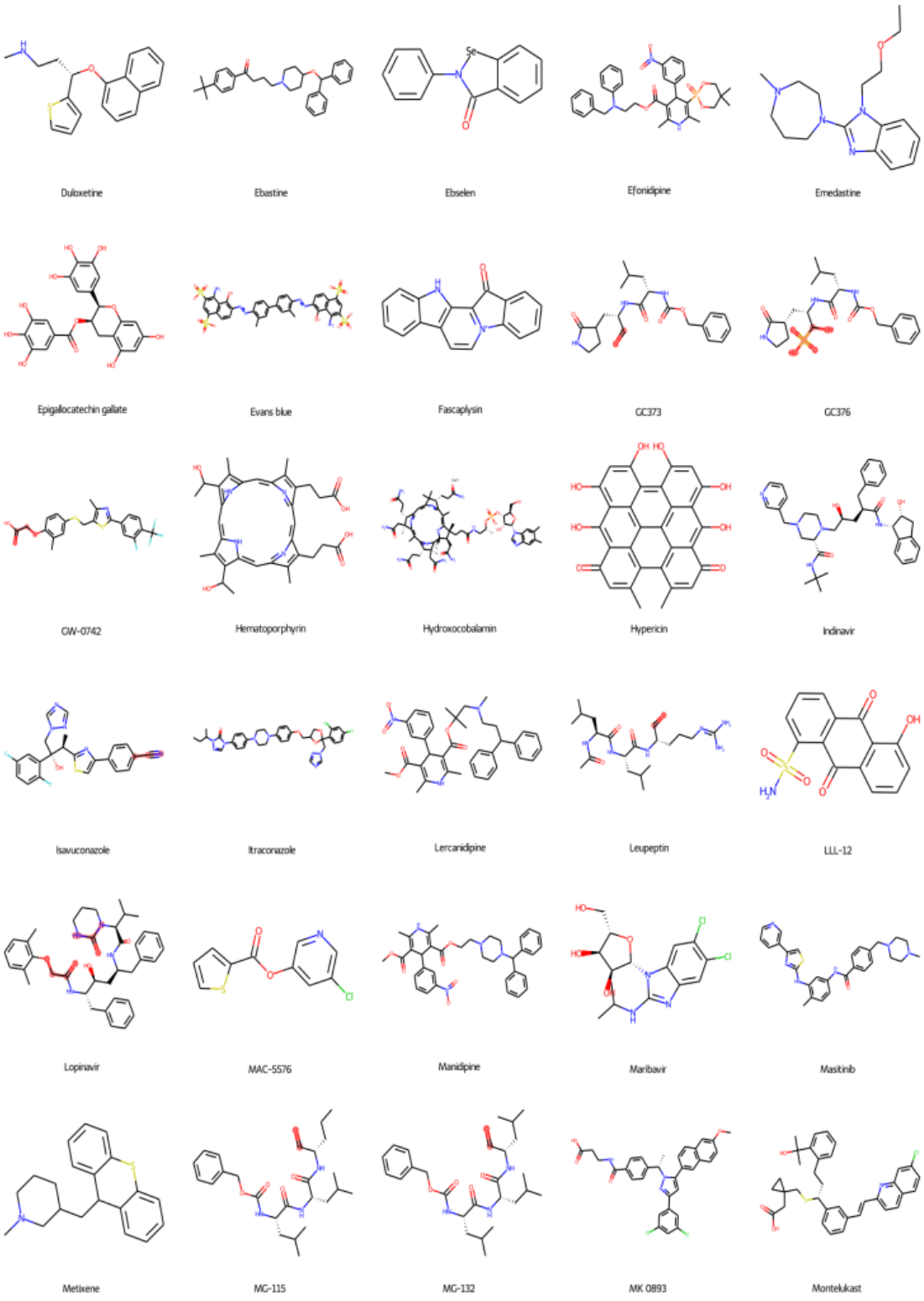
Duloxetine
Ebastine
Ebselen
Efonidipine
Emedastine
Epigallocatechin gallate
Evans blue
Fascaplysin
GC373
GC376
GW-0742
Hematoporphyrin
Hydroxocobalamin
Hypericin
Indinavir
Isavuconazole
Itraconazole
Lercanidipine
Leupeptin
LLL-12
Lopinavir
MAC-5576
Manidipine
Maribavir
Masitinib
Metixene
MG-115
MG-132
MK 0893
Montelukast

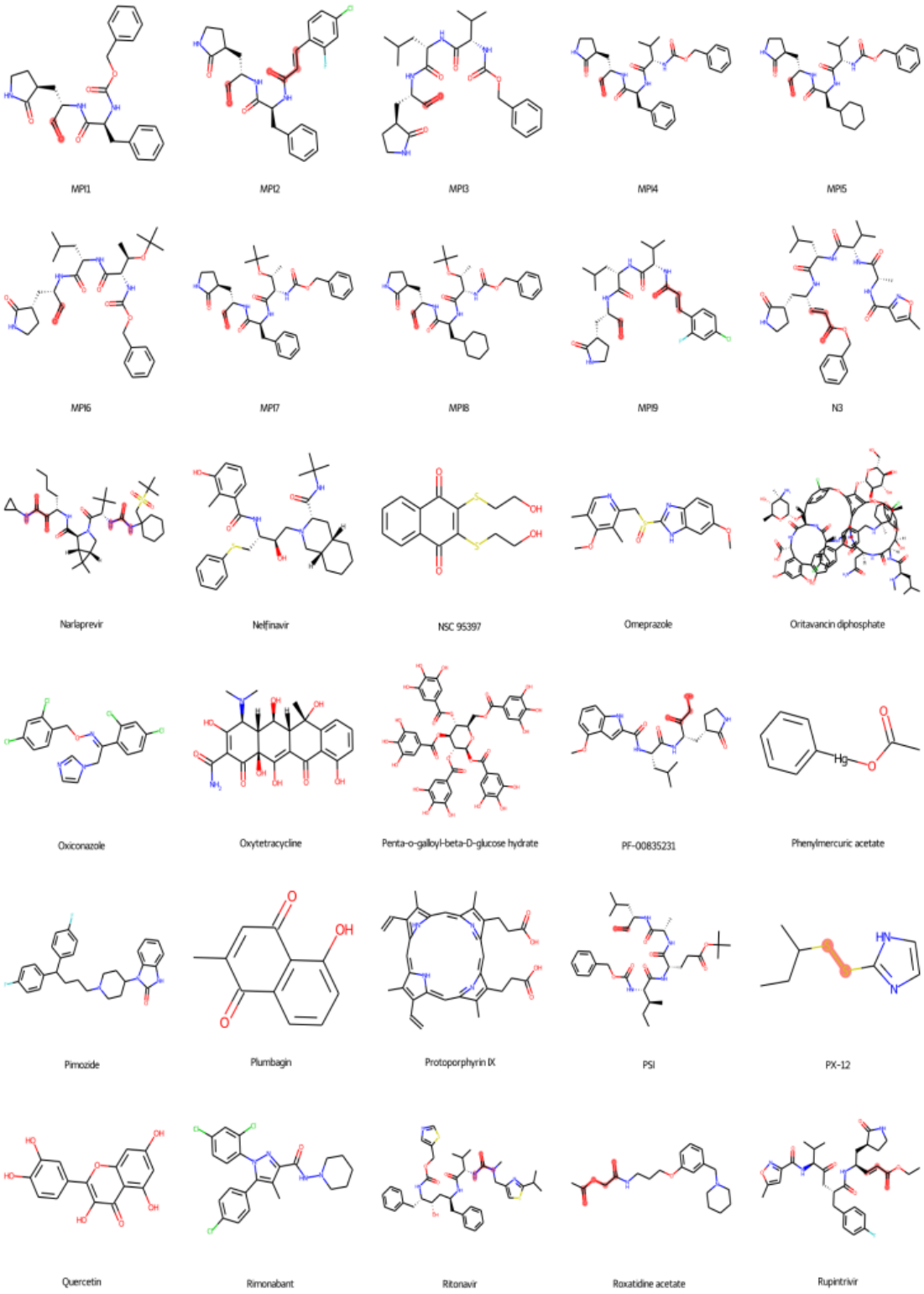
MPI1
MPI2
MPI3
MPI4
MPI5
MPI6
MPI7
MPI8
MPI9
N3
Narlaprevir
Nelfinavir
NSC 95397
Omeprazole
Oritavancin diphosphate
Oxiconazole
Oxytetracycline
Penta-o-galloyl-beta-D-glucose hydrate
PF-00835231
Phenylmercuric acetate
Pimozide
Plumbagin
Protoporphyrin IX
PSI
PX-12
Quercetin
Rimonabant
Ritonavir
Roxatidine acetate
Rupintrivir

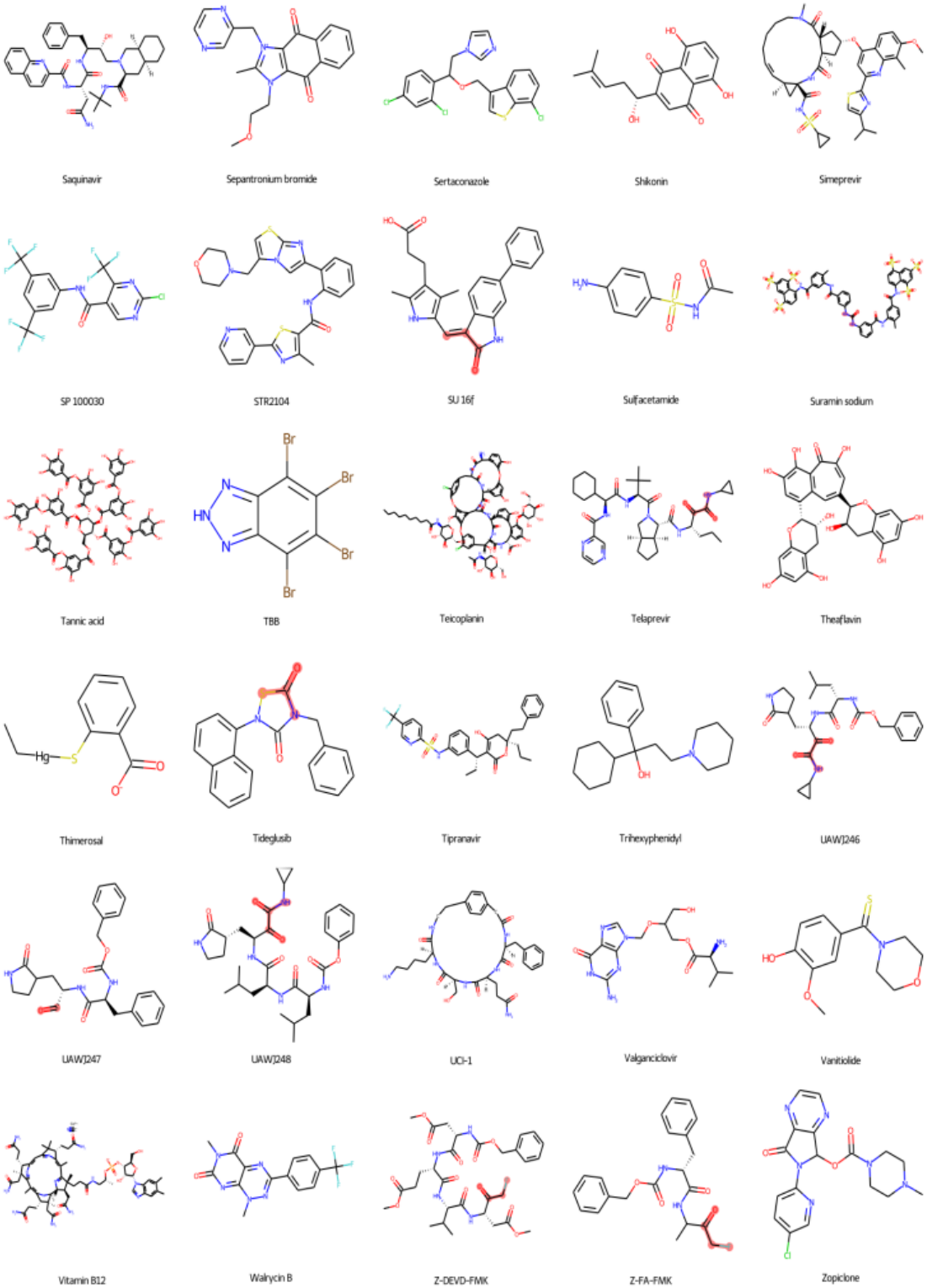
Saquinavir
Sepantronium bromide
Sertaconazole
Shikonin
Simeprevir
SP 100030
STR2104
SU 16f
Sulfacetamide
Suramin sodium
Tannic acid
TBB
Teicoplanin
Telaprevir
Theaflavin
Thimerosal
Tideglusib
Tipranavir
Trihexyphenidyl
UAWJ246
UAWJ247
UAWJ248
UCI-1
Valganciclovir
Vanitiolide
Vitamin B12
Wahrycin B
Z-DEVD-FMK
Z-FA-FMK
Zopiclone

Figure S2

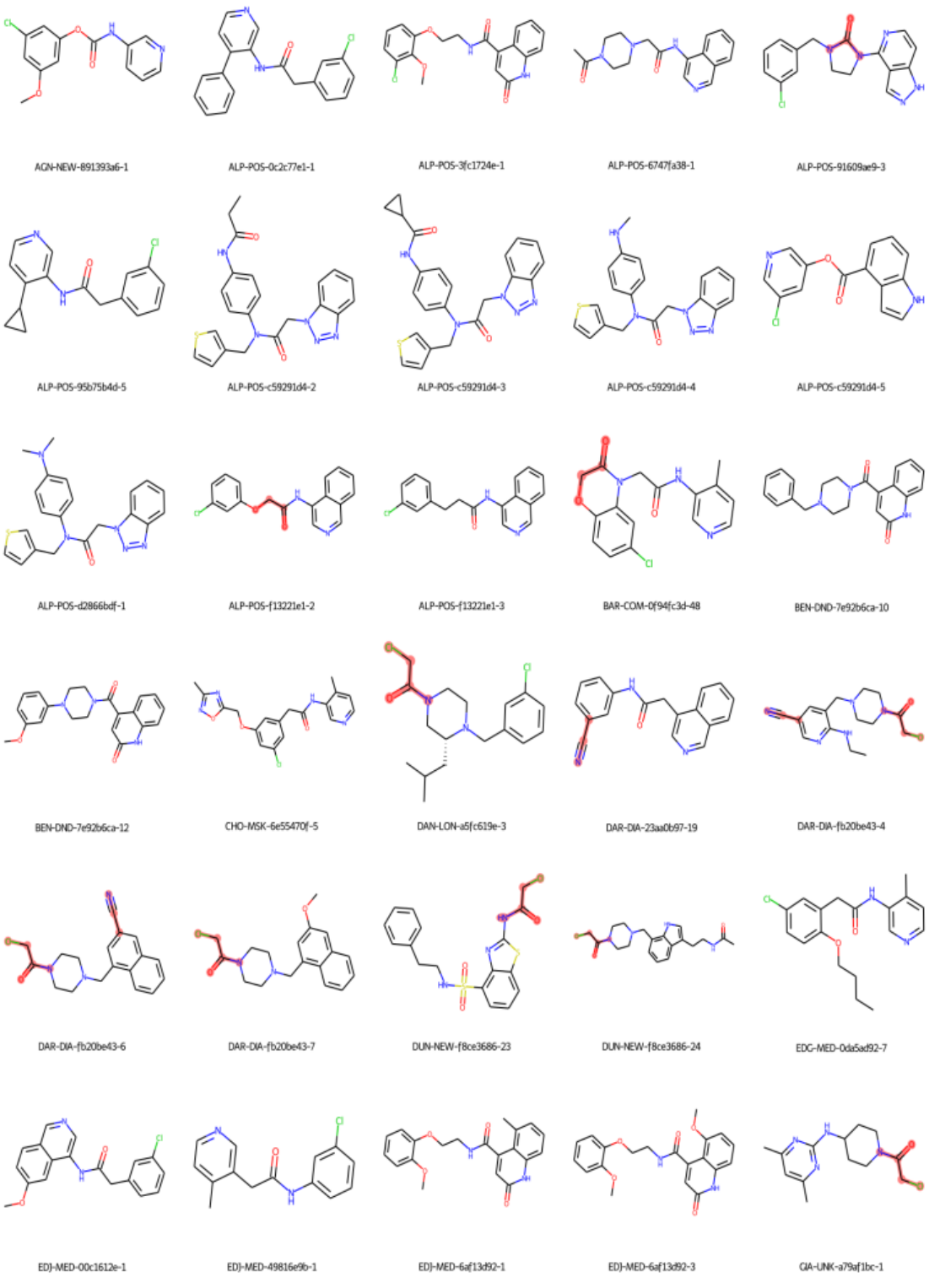
AGN-NEW-891393a6-1
ALP-POS-0c2c77e1-1
ALP-POS-3fc1724e-1
ALP-POS-6747fa38-1
ALP-POS-91609ae9-3
ALP-POS-95b75b4d-5
ALP-POS-c59291d4-2
ALP-POS-c59291d4-3
ALP-POS-c59291d4-4
ALP-POS-c59291d4-5
ALP-POS-d2866bdf-1
ALP-POS-f13221e1-2
ALP-POS-f13221e1-3
BAR-COM-0f94fc3d-48
BEN-DND-7e92b6ca-10
BEN-DND-7e92b6ca-12
CHO-MSK-6e55470f-5
DAN-LON-a5fc619e-3
DAR-DIA-23aa0b97-19
DAR-DIA-fb20be43-4
DAR-DIA-fb20be43-6
DAR-DIA-fb20be43-7
DUN-NEW-f8ce3686-23
DUN-NEW-f8ce3686-24
EDG-MED-0da5ad92-7
EDJ-MED-00c1612e-1
EDJ-MED-49816e9b-1
EDJ-MED-6af13d92-1
EDJ-MED-6af13d92-3
CIA-UNK-a79af1bc-1
Page 1 of 3

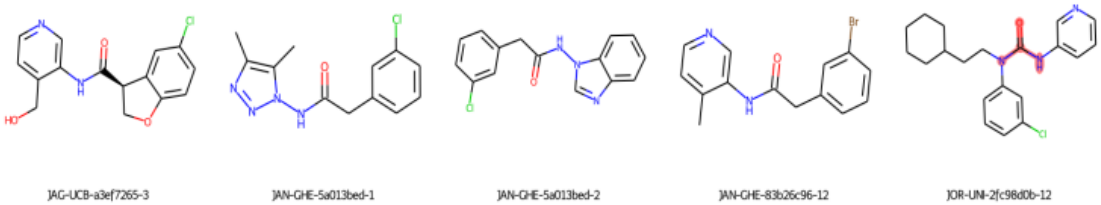

JAG-UCB-a3ef7265-3 JAN-GHE-5a013bed-1 JAN-GHE-5a013bed-2 JAN-GHE-83b26c96-12 JOR-UNI-2fc98d0b-12

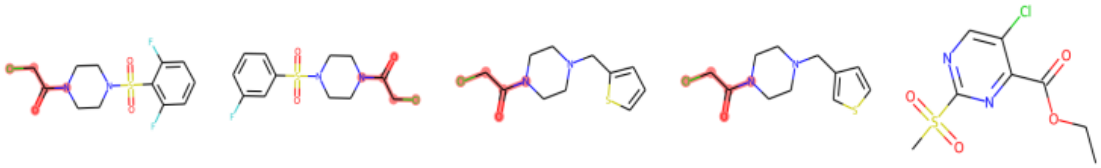

LON-WEI-8f408cad-2 LON-WEI-8f408cad-4 LON-WEI-8f408cad-5 LON-WEI-8f408cad-7 LON-WEI-ff7b210a-5

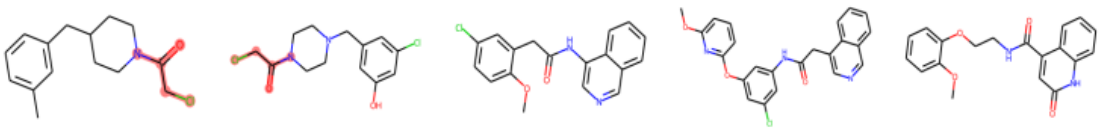

MAK-UNK-af83ef51-6 MAT-POS-2db6411e-2 MAT-POS-3b92565d-1 MAT-POS-6344a35d-1 MAT-POS-916a2c5a-2

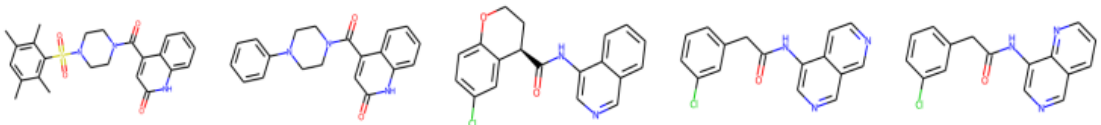

MAT-POS-916a2c5a-3 MAT-POS-916a2c5a-4 MAT-POS-b3e365b9-1 MAT-POS-bb423b95-1 MAT-POS-bb423b95-2

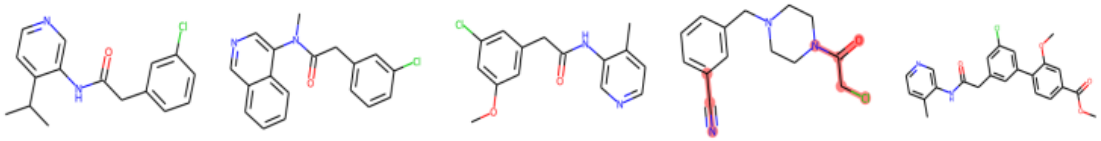

MAT-POS-bb423b95-5 MAT-POS-bb423b95-7 MAT-POS-c9973a83-1 MAT-POS-ee51dedd-1 MAT-POS-f42f3716-3

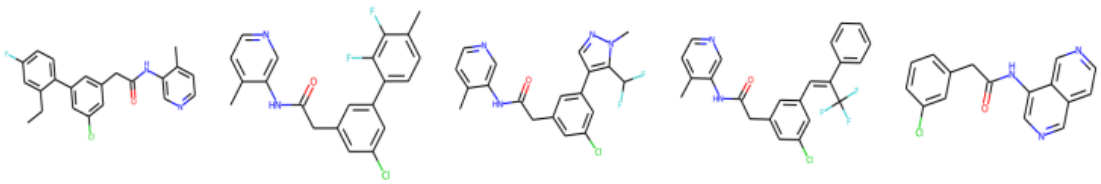

MAT-POS-f42f3716-4 MAT-POS-f42f3716-6 MAT-POS-f42f3716-7 MAT-POS-f42f3716-8 MAT-POS-f7918075-5

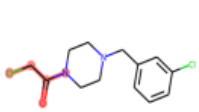

MED-COV-4280ac29-15

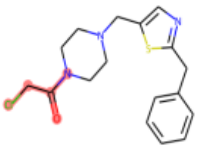

MED-COV-4280ac29-25

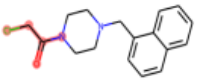

MED-COV-4280ac29-31

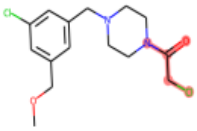

MED-COV-4280ac29-33

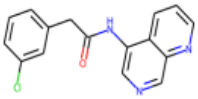

MIC-UNK-08cd9c58-1

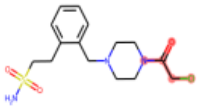

MIH-UNI-e573136b-5

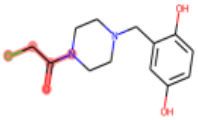

NEH-REV-107bcf72-5

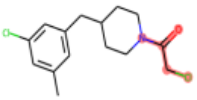

NIR-THE-0d6461ce-8

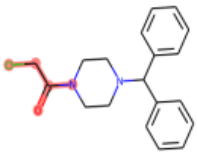

SIM-SYN-f15aaa3a-1

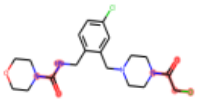

STU-CHA-6cae54d3-1

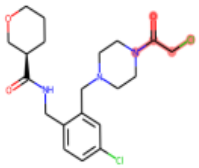

STU-CHA-7b3b91d5-1

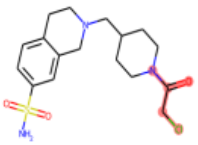

STU-CHA-83dacf15-1

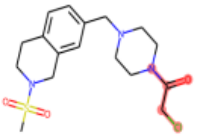

TAM-UNI-d1c3dd9f-5

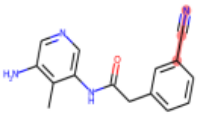

TRY-UNI-714a760b-19

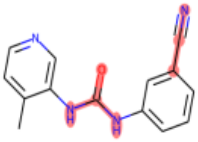

TRY-UNI-714a760b-24

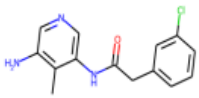

TRY-UNI-714a760b-3

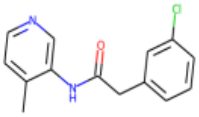

TRY-UNI-714a760b-6

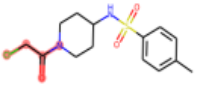

WAR-XCH-79d12f6e-4

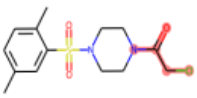

WAR-XCH-79d12f6e-6

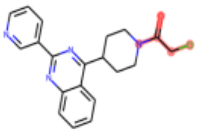

WAR-XCH-b0339bbe-19

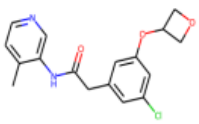

WIL-MOO-03b86a88-4

Figure S3

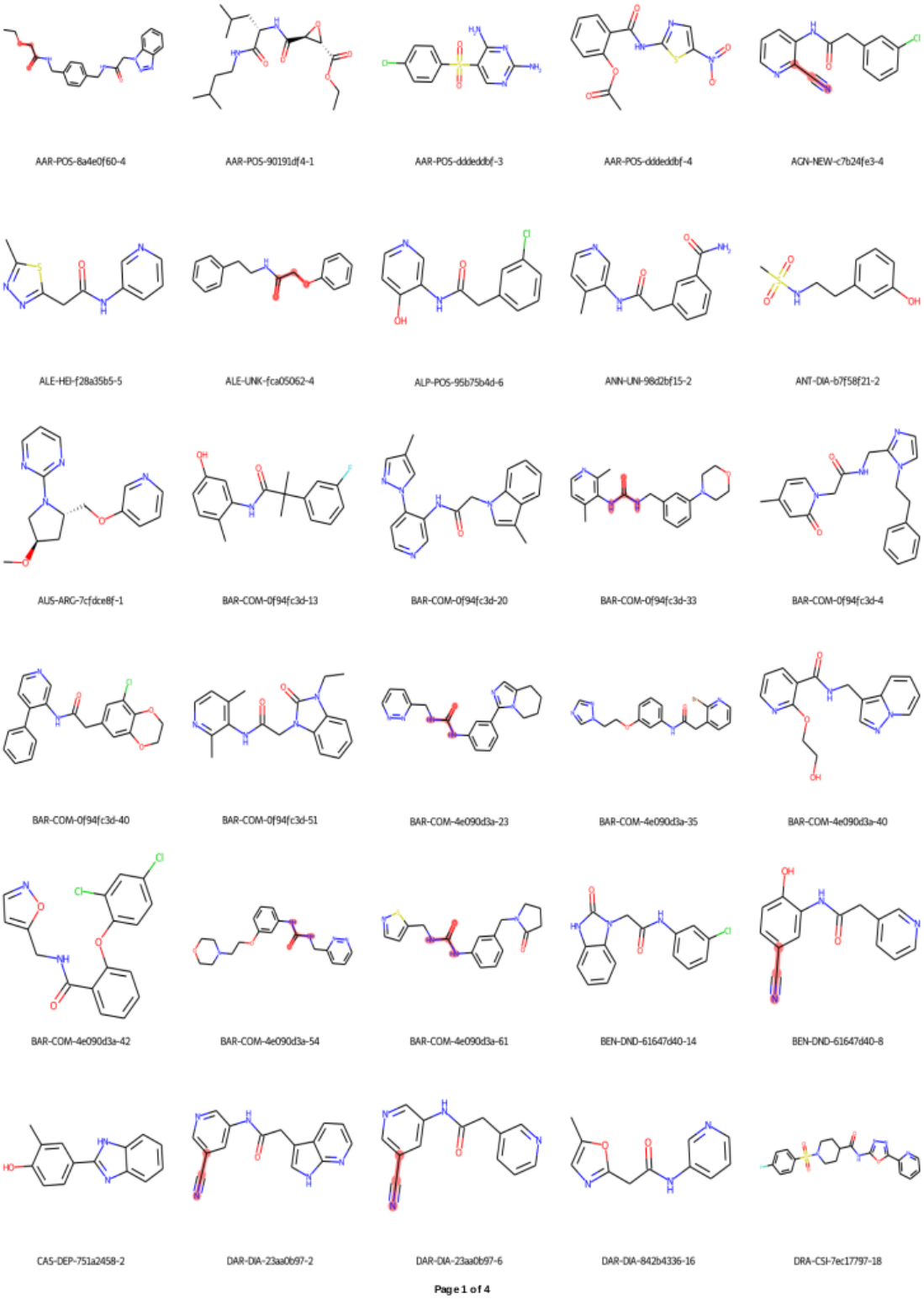
AAR-POS-8a4e0f60-4
AAR-POS-90191df4-1
AAR-POS-ddddeddbf-3
AAR-POS-ddddeddbf-4
ACN-NEW-c7b24fe3-4
ALE-HEI-f28a35b5-5
ALE-UNK-fca05062-4
ALP-POS-95b75b4d-6
ANN-UNI-98d2bf15-2
ANT-DIA-b7f58f21-2
AUS-ARG-7cfdce8f-1
BAR-COM-0f94fc3d-13
BAR-COM-0f94fc3d-20
BAR-COM-0f94fc3d-33
BAR-COM-0f94fc3d-4
BAR-COM-0f94fc3d-40
BAR-COM-0f94fc3d-51
BAR-COM-4e090d3a-23
BAR-COM-4e090d3a-35
BAR-COM-4e090d3a-40
BAR-COM-4e090d3a-42
BAR-COM-4e090d3a-54
BAR-COM-4e090d3a-61
BEN-DND-61647d40-14
BEN-DND-61647d40-8
CAS-DEP-751a2458-2
DAR-DIA-23aa0b97-2
DAR-DIA-23aa0b97-6
DAR-DIA-842b4336-16
DRA-CSI-7ec17797-18
Page 1 of 4

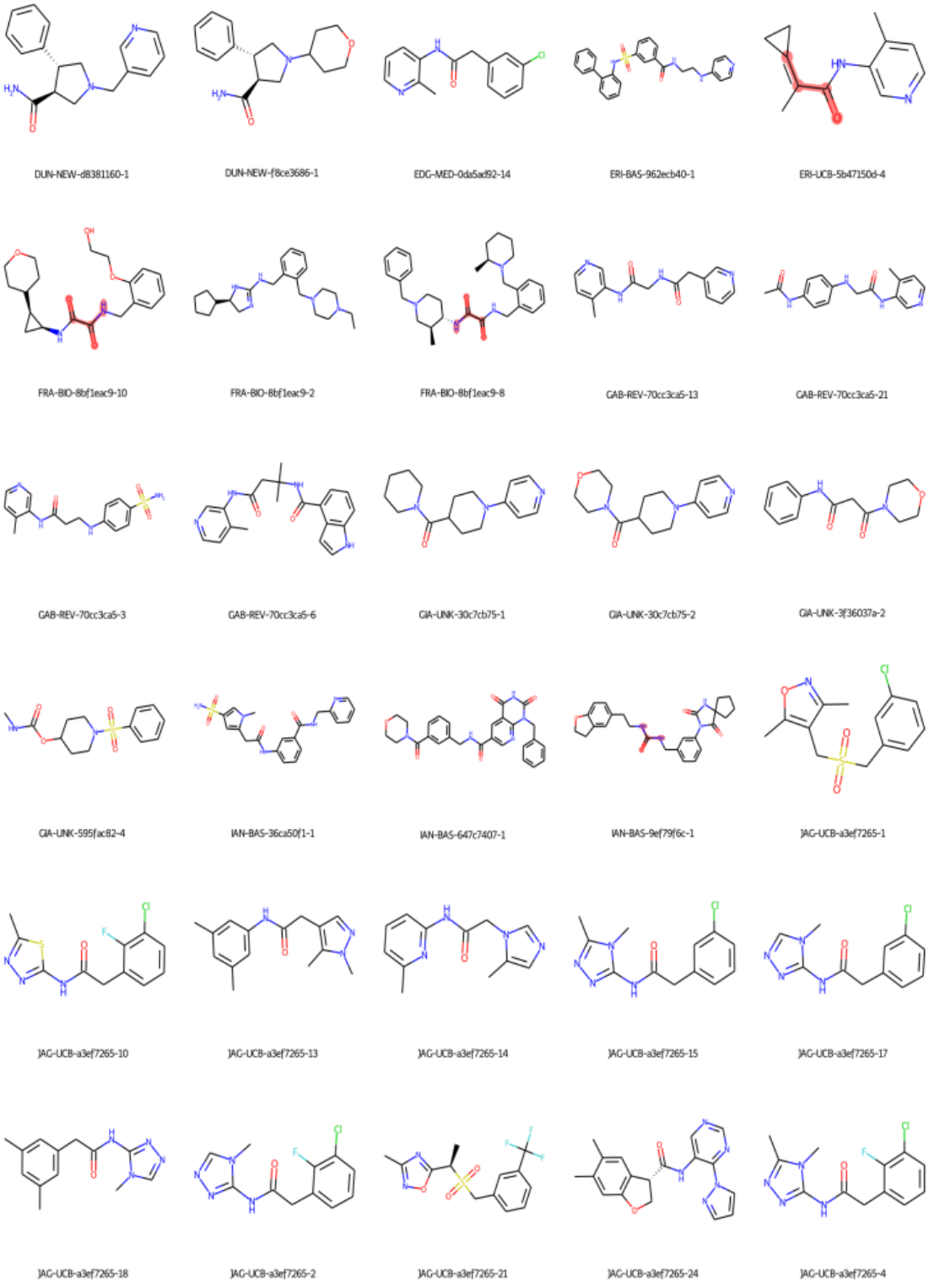
DUN-NEW-d8381160-1
DUN-NEW-f8ce3686-1
EDG-MED-0da5ad92-14
ERI-BAS-962ecb40-1
ERI-UCB-5b47150d-4
FRA-BIO-8bf1eac9-10
FRA-BIO-8bf1eac9-2
FRA-BIO-8bf1eac9-8
GAB-REV-70cc3ca5-13
GAB-REV-70cc3ca5-21
GAB-REV-70cc3ca5-3
GAB-REV-70cc3ca5-6
GIA-UNK-30c7cb75-1
GIA-UNK-30c7cb75-2
GIA-UNK-3f36037a-2
GIA-UNK-595fac82-4
IAN-BAS-36ca50f1-1
IAN-BAS-647c7407-1
IAN-BAS-9ef79f6c-1
JAG-UCB-a3ef7265-1
JAG-UCB-a3ef7265-10
JAG-UCB-a3ef7265-13
JAG-UCB-a3ef7265-14
JAG-UCB-a3ef7265-15
JAG-UCB-a3ef7265-17
JAG-UCB-a3ef7265-18
JAG-UCB-a3ef7265-2
JAG-UCB-a3ef7265-21
JAG-UCB-a3ef7265-24
JAG-UCB-a3ef7265-4
Page 2 of 4

JAG-UCB-a3ef7265-6

JAG-UCB-a3ef7265-9

JAG-UCB-cedd89ab-3

JAG-UCB-ef2c0e8e-10

JAG-UCB-ef2c0e8e-3

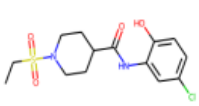

JAG-UCB-ef2c0e8e-6

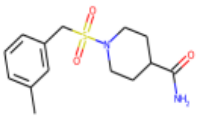

JAG-UCB-ef2c0e8e-8

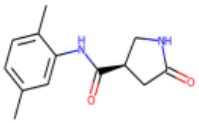

JAG-UCB-ef2c0e8e-9

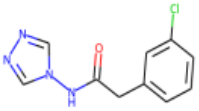

JAN-GHE-5a013bed-5

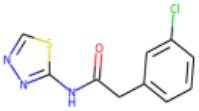

JAN-GHE-5a013bed-7

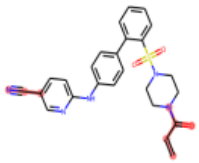

JAN-GHE-bf40f168-2

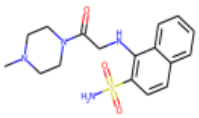

JAR-KUA-672ec752-3

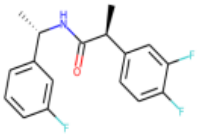

JON-UIO-066ce08b-7

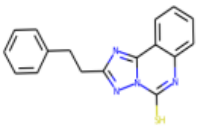

LON-WEI-ff7b210a-7

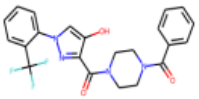

LON-WEI-ff7b210a-9

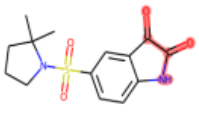

LOR-NEU-c8f11034-8

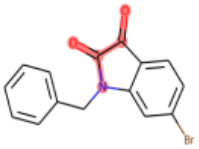

LOR-NEU-c8f11034-9

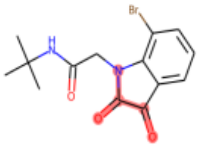

LOR-NOR-30067bb9-12

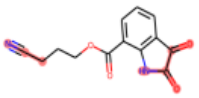

LOR-NOR-30067bb9-16

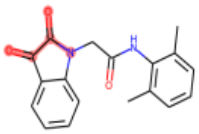

LOR-NOR-30067bb9-17

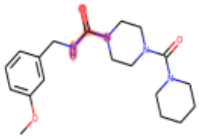

LUI-IND-2c46affe-3

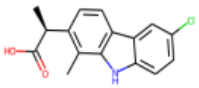

MAK-UNK-0d6072ac-20

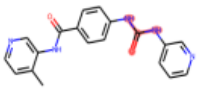

MAK-UNK-129dcd6f-12

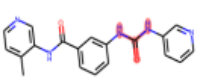

MAK-UNK-129dcd6f-9

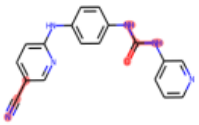

MAK-UNK-30aad1f1-12

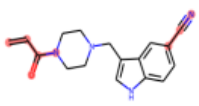

MAT-POS-2db6411e-1

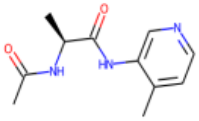

MAT-POS-590ac91e-13

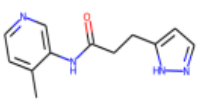

MAT-POS-590ac91e-17

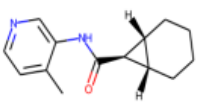

MAT-POS-590ac91e-19

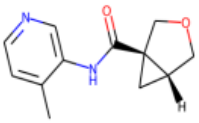

MAT-POS-590ac91e-3

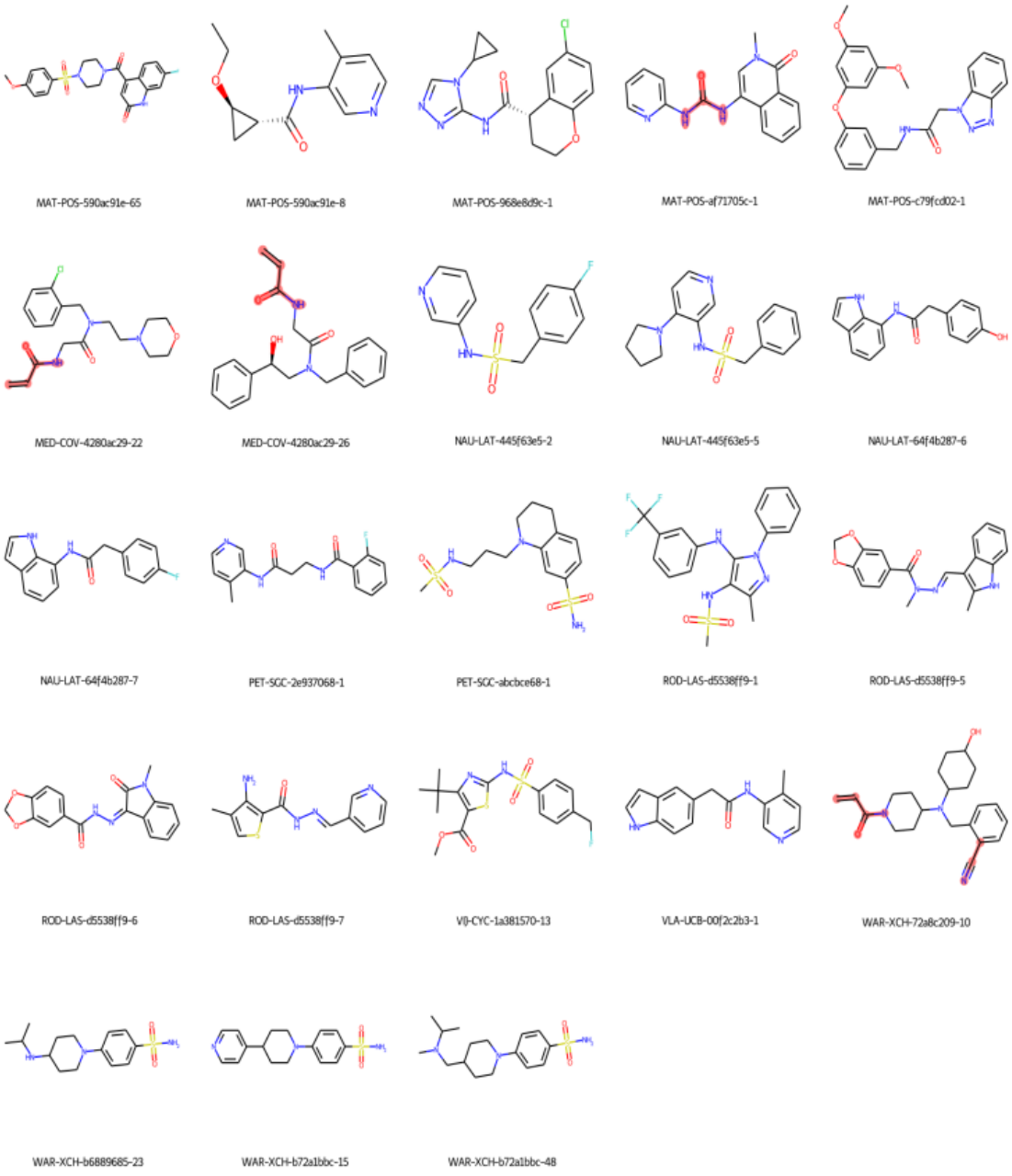
MAT-POS-590ac91e-65
MAT-POS-590ac91e-8
MAT-POS-968e8d9c-1
MAT-POS-af71705c-1
MAT-POS-c79fcd02-1
MED-COV-4280ac29-22
MED-COV-4280ac29-26
NAU-LAT-445f63e5-2
NAU-LAT-445f63e5-5
NAU-LAT-64f4b287-6
NAU-LAT-64f4b287-7
PET-SGC-2e937068-1
PET-SGC-abcbce68-1
ROD-LAS-d5538ff9-1
ROD-LAS-d5538ff9-5
ROD-LAS-d5538ff9-6
ROD-LAS-d5538ff9-7
V0-CYC-1a381570-13
VLA-UCB-00f2c2b3-1
WAR-XCH-72a8c209-10
WAR-XCH-b6889685-23
WAR-XCH-b72a1bbc-15
WAR-XCH-b72a1bbc-48

Figure S4

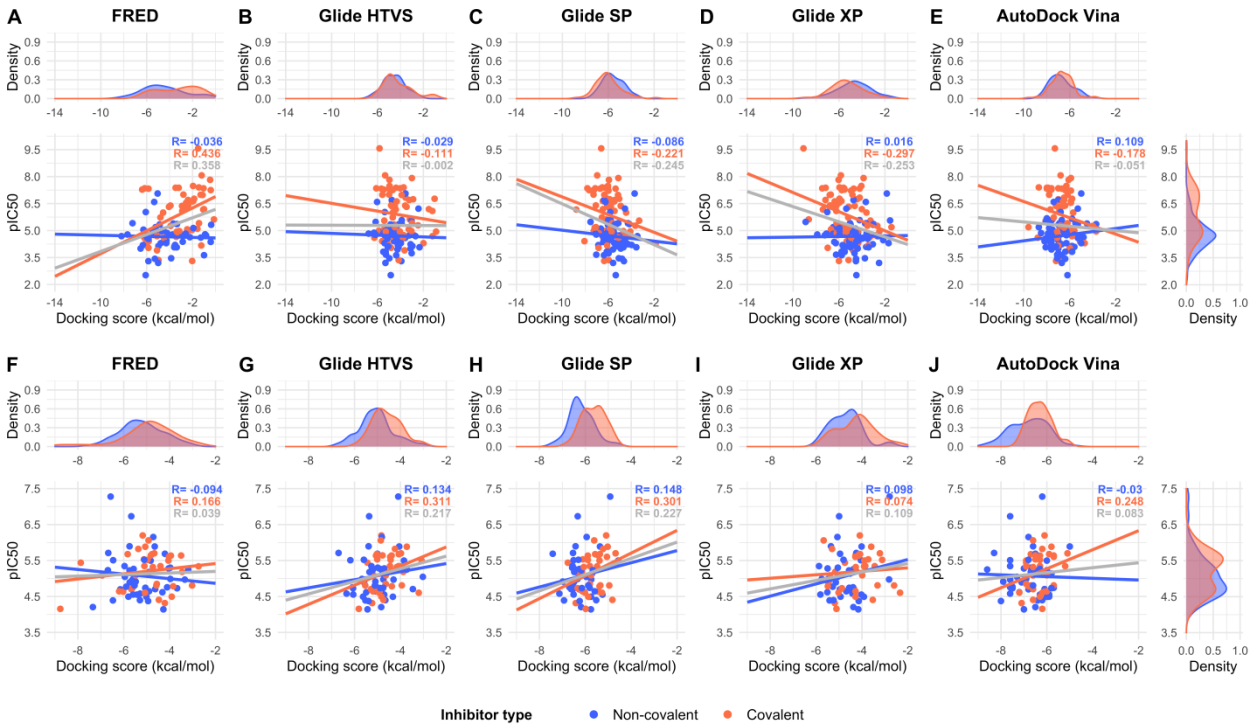
A FRED
B Glide HTVS
C Glide SP
D Glide XP
E AutoDock Vina
F FRED
G Glide HTVS
H Glide SP
I Glide XP
J AutoDock Vina
Density
pIC50
Docking score (kcal/mol)
R= -0.036
R= 0.436
R= 0.358
R= -0.029
R= -0.111
R= -0.002
R= -0.086
R= -0.221
R= -0.245
R= 0.016
R= -0.297
R= -0.253
R= 0.109
R= -0.178
R= -0.051
R= -0.094
R= 0.166
R= 0.039
R= 0.134
R= 0.311
R= 0.217
R= 0.148
R= 0.301
R= 0.227
R= 0.098
R= 0.074
R= 0.109
R= -0.03
R= 0.248
R= 0.083
Inhibitor type
Non-covalent
Covalent

Figure S5

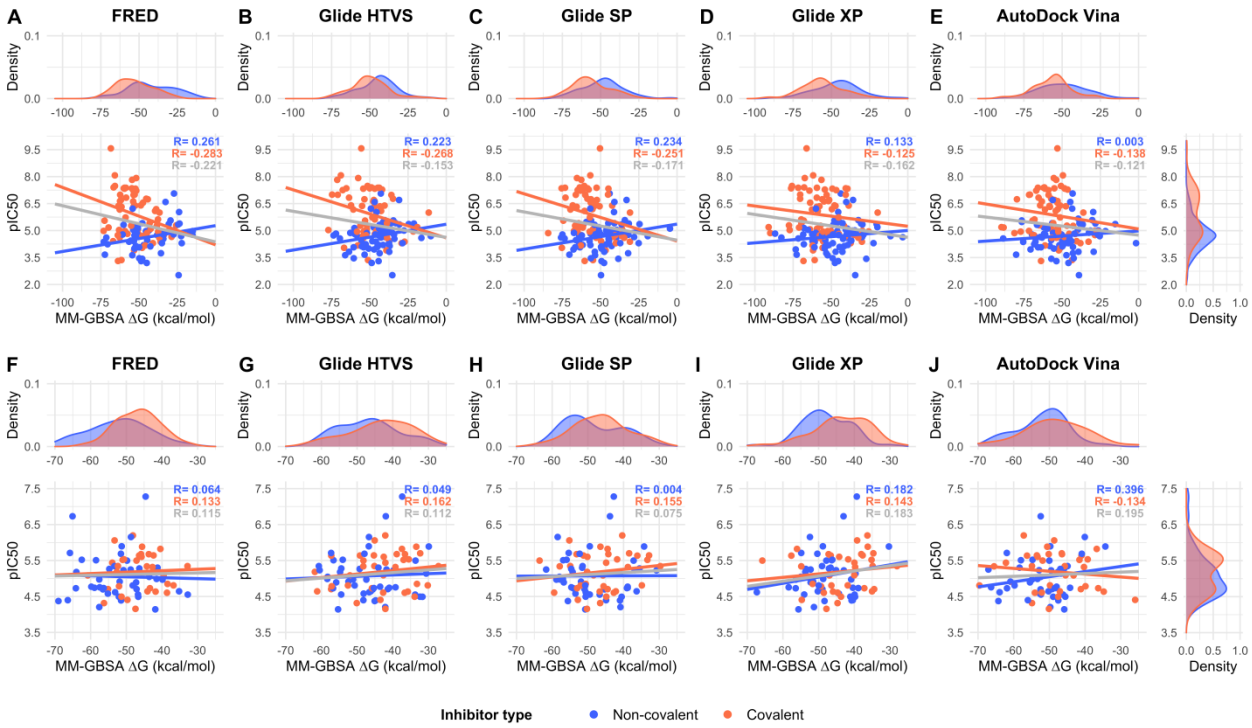
A FRED
B Glide HTVS
C Glide SP
D Glide XP
E AutoDock Vina
F FRED
G Glide HTVS
H Glide SP
I Glide XP
J AutoDock Vina
Density
pIC50
MM-GBSA ΔG (kcal/mol)
R= 0.261
R= -0.283
R= -0.221
R= 0.223
R= -0.268
R= -0.153
R= 0.234
R= -0.251
R= -0.171
R= 0.133
R= -0.125
R= -0.162
R= 0.003
R= -0.138
R= -0.121
R= 0.064
R= 0.133
R= 0.115
R= 0.049
R= 0.162
R= 0.112
R= 0.004
R= 0.155
R= 0.075
R= 0.182
R= 0.143
R= 0.183
R= 0.396
R= -0.134
R= 0.195
Inhibitor type
Non-covalent
Covalent

Figure S6

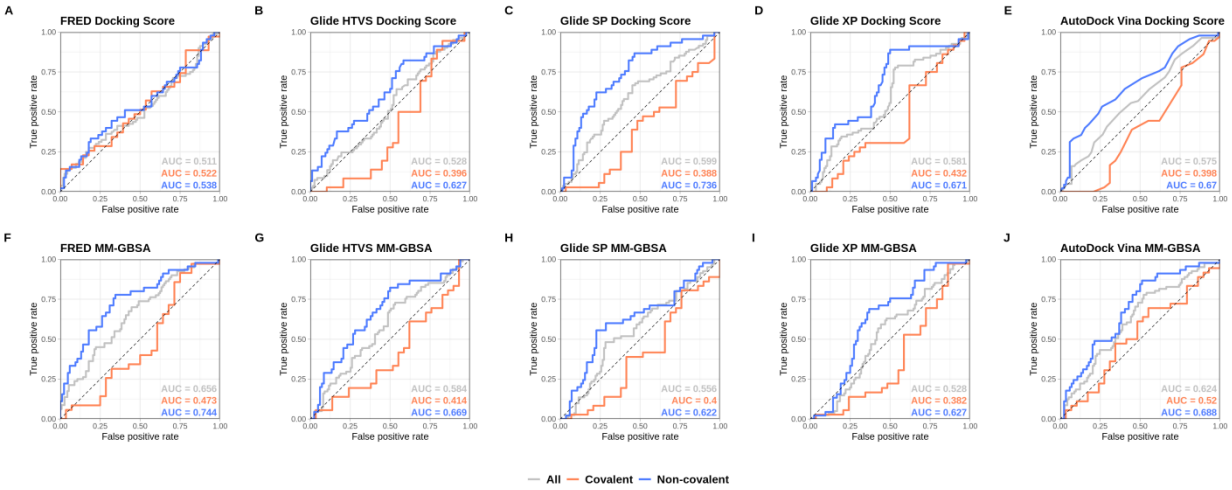
A
FRED Docking Score
AUC = 0.511
AUC = 0.522
AUC = 0.538
B
Glide HTVS Docking Score
AUC = 0.528
AUC = 0.396
AUC = 0.627
C
Glide SP Docking Score
AUC = 0.599
AUC = 0.388
AUC = 0.736
D
Glide XP Docking Score
AUC = 0.581
AUC = 0.432
AUC = 0.671
E
AutoDock Vina Docking Score
AUC = 0.575
AUC = 0.398
AUC = 0.67
F
FRED MM-GBSA
AUC = 0.656
AUC = 0.473
AUC = 0.744
G
Glide HTVS MM-GBSA
AUC = 0.584
AUC = 0.414
AUC = 0.669
H
Glide SP MM-GBSA
AUC = 0.556
AUC = 0.4
AUC = 0.622
I
Glide XP MM-GBSA
AUC = 0.528
AUC = 0.382
AUC = 0.627
J
AutoDock Vina MM-GBSA
AUC = 0.624
AUC = 0.52
AUC = 0.688
True positive rate
False positive rate
All
Covalent
Non-covalent

Figure S7

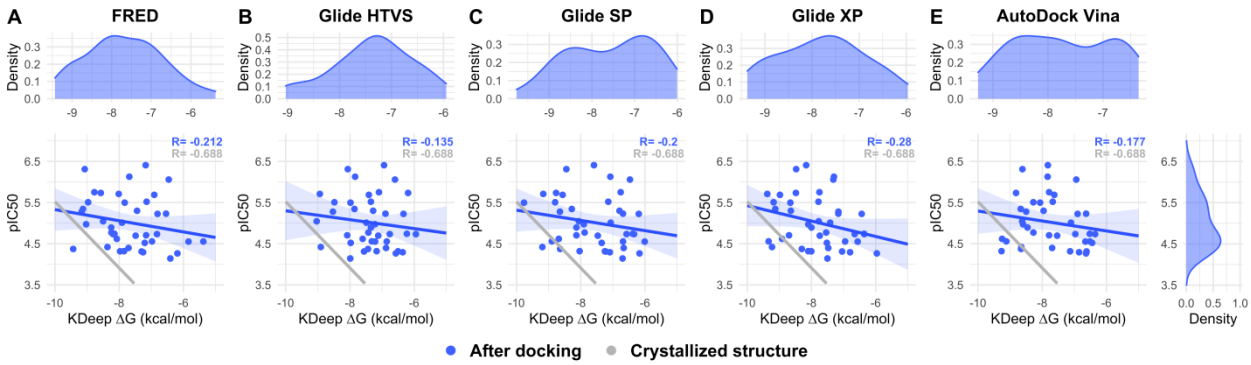
A
FRED
B
Glide HTVS
C
Glide SP
D
Glide XP
E
AutoDock Vina
Density
pIC50
KDeep ΔG (kcal/mol)
R= -0.212
R= -0.688
R= -0.135
R= -0.688
R= -0.2
R= -0.688
R= -0.28
R= -0.688
R= -0.177
R= -0.688
After docking
Crystallized structure